



**Organic Nanophotonics: from Controllable Self-Assembly of
Optofunctional Molecules to Low-Dimensional Materials
with Desired Photonic Properties**

Journal:	<i>Chemical Society Reviews</i>
Manuscript ID:	CS-TRV-03-2014-000098
Article Type:	Tutorial Review
Date Submitted by the Author:	03-Mar-2014
Complete List of Authors:	Yan, Yongli; Institute of Chemistry, Chinese Academy of Sciences, The Center of Molecular Science Zhao, Yong Sheng; Institute of Chemistry, Chinese Academy of Sciences,

Key learning points:

- (1) Self-assembly characteristics of small organic molecules
- (2) The dependence of organic nanostructures on the molecular assembly
- (3) Photonic properties of organic nanomaterials with specific structures and compositions
- (4) Function-guided material design and synthesis through molecular tailoring

Graphical and Textual Abstract

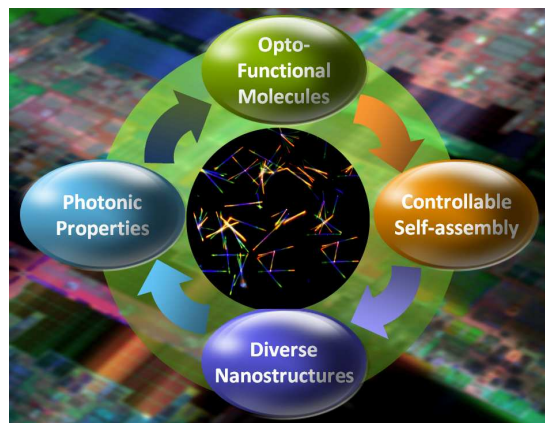
Organic Nanophotonics: from Controllable Self-Assembly 5 of Optofunctional Molecules to Low-Dimensional Materials with Desired Photonic Properties

Yongli Yan and Yong Sheng Zhao*

10 The tutorial review aims to provide an insight into the relationship among opto-functional molecules, controllable self-assembly, diverse nanostructures and photonic properties, which can further guide the function-oriented design and synthesis of low-dimensional materials for integrated photonic devices.

15

20



25

Cite this: DOI: 10.1039/c0xx00000x

www.rsc.org/xxxxxx

Tutorial Review

Organic Nanophotonics: from Controllable Self-Assembly of Optofunctional Molecules to Low-Dimensional Materials with Desired Photonic Properties

Yongli Yan and Yong Sheng Zhao*

5 Received (in XXX, XXX) Xth XXXXXXXXX 20XX, Accepted Xth XXXXXXXXX 20XX
DOI: 10.1039/b000000x

Nanophotonics, that mainly studies the behavior of light-matter interaction at the wavelength scale, has developed into one of the most important branches in optics-related disciplines. Utilizing organic functional molecules as the building blocks of nanophotonic materials and devices exhibits great potentials due to the multiple advantages, including the molecular designability, good processability, tailorable properties, and so on. Small molecules exhibit a strong tendency to aggregate into low-dimensional structures through self-assembly process. The morphologies of the formed products, which are tightly related to the stacking modes of the molecules, can be precisely controlled through the modulation of various intermolecular interactions. The optical properties of organic complex structures, self-assembled from one or more types of small molecules, show heavy dependences on the composition, distribution, as well as the topological structures, manifesting a strategy to acquiring desired photonic properties via rational structural design and/or componential modulation. This tutorial review focuses on the relationship among various molecules, diverse structures and photonic properties, with emphases on the controllable self-assembly processes to low-dimensional structures and self-assembly strategy to requisite optofunctional properties.

1. Introduction

Nanophotonics, that is the generation, transfer, modulation and detection of photons in a confined system, was first used in the field of near-field optics/spectroscopy, and subsequently generalized in other fields such as photonic crystals and surface plasmon optics.¹ Since photon exhibits great superiority over electron as information carrier, including speed, bandwidth, capacity, *etc.*, nanophotonics provides a promising solution to the current bottlenecks that limit the further improvement of modern electronics. Therefore, the photonic applications of inorganic/organic nanostructures become a relatively new branch of nanophotonics. There is no existing guidance for the design of photonic materials and devices due to the vast differences between photon and electron in fundamental physical properties at the moment. Chemists and material scientists, in this respect, have made an outstanding contribution in achieving novel optical properties with inorganic materials, such as ZnO, CdSe as well as noble metal nanostructures.² During the flourish of their inorganic counterpart, organics are gradually becoming a better choice as nanophotonic materials due to numerous advantages. Organic molecules possess high photoluminescence quantum yields, tunable optical properties, and rapid photoresponses. The excellent flexibility and processability are also big pluses in the fabrication of functional photonic devices. Taken together, it is no doubt that organic molecular materials are good candidates for the design and fabrication of functional elements towards

photonic integrated circuits.³

Organic compounds, especially small molecules, tend to form crystalline structures through self-assembly process driven by the weak interactions among the molecules, such as hydrogen bond, Van der Waals' force, π - π interaction, *etc.*⁴ These weak intermolecular interactions allow for more facile and mild conditions in the fabrication of high quality low-dimensional structures. There have been numerous efforts in the synthesis of organic nanostructures through a variety of methods, including self-assembly in liquid phase, epitaxial growth in vapor phase and template-involved methods.⁵ It is indicated that molecular interactions play an important role in dominating the self-assembly characteristics.⁶ In general, participation of a single force will cause a molecular packing along a preferential direction and result in one-dimensional (1D) structures. The participation of two or more kinds of interactions will complicate the self-assembly process and nanostructures with various morphologies are expectable. It is necessary to summarize the relationship between the intermolecular interactions and the final structural features to further guide the molecular design and construction strategy optimization.

One of the most important reasons why organic nanomaterials become so attractive is their unique optical properties, which is fundamentally different from the inorganic division.⁷ The optical properties of self-assembled nanostructures depend not only on those of molecules themselves, but also on the morphologies of their aggregates.⁸ Aggregation induced enhanced

photoluminescence,⁹ mainly because of the reduced vibration-rotation in solid state, has been reported in plenty of molecules. In addition, those as-prepared crystalline structures with regular shapes are often accompanied with remarkable photon confinements, including but not limiting to cavity effect and waveguide behavior. Moreover, the formation of exciton polaritons (EPs), that is the strong coupling between photon and Frenkel type exciton, can change the original properties a lot and cause plenty of new phenomena.¹⁰ The fruitful excited state processes among different molecules, *i.e.* energy/charge transfer, exciton diffusion, separation and recombination¹¹ could bring much flexibility in the realization of complex photonic functions. Therefore, a thorough understanding of relationship between optical properties and structures is essential to direct the material design and synthesis.

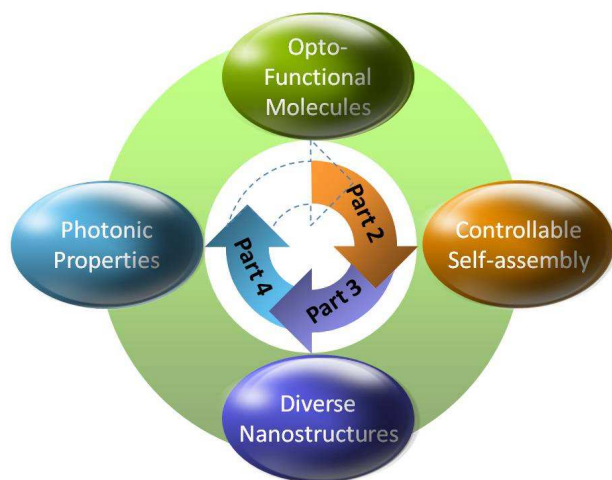


Fig.1 Organization of this review. Part 2: molecular self-assembly characteristics, which are determined by intermolecular interactions. Part 3: low-dimensional structures with diverse morphologies through the controllable self-assembly processes. Part 4: Optical properties and photonic applications of the self-assembled complex structures.

In this tutorial review, we mainly focus on the relationships among molecules, self-assembly characteristics, structures and photonic properties, which are divided into three parts (Figure 1). We start by looking at how opto-functional molecules begin to self-assemble under various intermolecular forces (Part 2). Then, we put emphases on the relationship between self-assembly behavior and morphologies of the final low-dimensional structures, providing a way to fabricate diverse nanostructures through rational control of intermolecular interactions (Part 3). In the following part, we will concentrate on the structural design and corresponding cooperative self-assembly method of multiple molecules towards complex photonic functions and high performance (Part 4). Finally, we summarize the recent contributions as well as significances in this field and put forward the prospects and directions for future development.

2. From molecules to self-assembly

The development of a facile construction strategy to organic low-dimension structures is a crucial prerequisite to the further investigation of optofunctions. Present methods to inorganic materials are not suitable for organic categories because of the

vicious reaction conditions, such as high pressure, high temperature, and various solvent. Fortunately, some meaningful attempts for synthesizing organic materials have been made in the past couple of years. Self-assembly has been demonstrated to be a facile and universal route to organic solid materials.¹² This bottom-up method starts from the aggregation of individual molecule, and ends up with dynamic balance in liquid phase or depletion of raw materials in vapor phase.

Molecules could self-assemble into crystals on some occasions if the nucleation and crystal growth processes coexist in a system. The tiny aggregations self-assembled at the initial stage can serve as stable nuclei once they reach a critical size. Then the crystals grow larger and larger until the whole system reaches equilibrium. The fundamental difference between self-assembly and crystallization processes is the driving forces. The crystallization process, which consists of nucleation and crystal growth stages, was driven by supersaturation, while the driving forces behind self-assembly process may come from the inherent weak intermolecular interactions or the influences from the environments. Here we elaborate on how these interactions impact on the molecular behavior in the self-assembly process.

2.1 Inherent intermolecular interactions

Among numerous construction strategies for organic micro-nanostructured materials, the most widespread one is self-assembly in liquid phase, because of the simplification and flexibility. By carefully managing the self-assembly behavior, people can obtain regular-shaped aggregates. For small molecules, the weak interactions among molecules, that usually are one or more kinds of π - π interaction, Van der Waals' force, hydrogen bond, *etc.*, play a key role in promoting the aggregation behavior. Continuous efforts have been made to explore the relationship between the interactions and the pattern modes of molecules in crystalline structures with smooth surfaces and flat end facets.

Figure 2 summarizes several typical molecular structures (fibers, tube, sheet and ring) fabricated through the self-assembly behavior of organic molecules. Shown in Figure 2A is a representative formation mechanism of the nanowires, which are self-assembled from a π -conjugated compound, 2-(N,N-diethylanilin-4-yl)-4,6-bis(3,5-dimethylpyrazol-1-yl)-1,3,5-triazine (DBPT).¹³ It is known from Figure 2A middle that the molecule has a preferential stacking direction along the *c* crystal axis because of the strong π - π interaction stemming from the middle core. Therefore DBPT molecules stack one by one along the [001] direction, leading to the formation of 1D nanostructures. The SEM image displayed in Figure 2A (right) further confirms that the 1D wire-like structures growing along a single direction are smooth-surfaced. The flat end facets can serve as reflectors to form high quality Fabry-Pérot cavities.

Things change if there is more than one kind of interactions during self-assembly. Figure 2B schematically elucidates of the formation mechanism of a tubular structure from a novel back-to-back coupled 2,6-di-pyrazol-1-ylpyridine compound,¹⁴ whose structure is show in Figure 2B. The molecule is near planar (demonstrated by the optimized top view and side view images). The hydrogen bond formed by pyrazole-ring nitrogen and pyrazole-ring proton facilitates a head-to-tail packing pattern and thus form a 1D chain like structure, which is then closely packed

and forms a pseudo sheet-like structure. These sheet-like structures could aggregate into 3D multilayered supramolecular structure via intermolecular π - π interactions of the pyridine rings. The supramolecular aggregates are not thermodynamically stable, and an unfolding of 90 degree along the sheet axis was found to

minimize the surface energy. After a subsequent seaming process, these triple folded nanosheets formed a rectangular tube-like structure. The further growth of the tube along the axis was steered by the rapid growth of the tube walls.

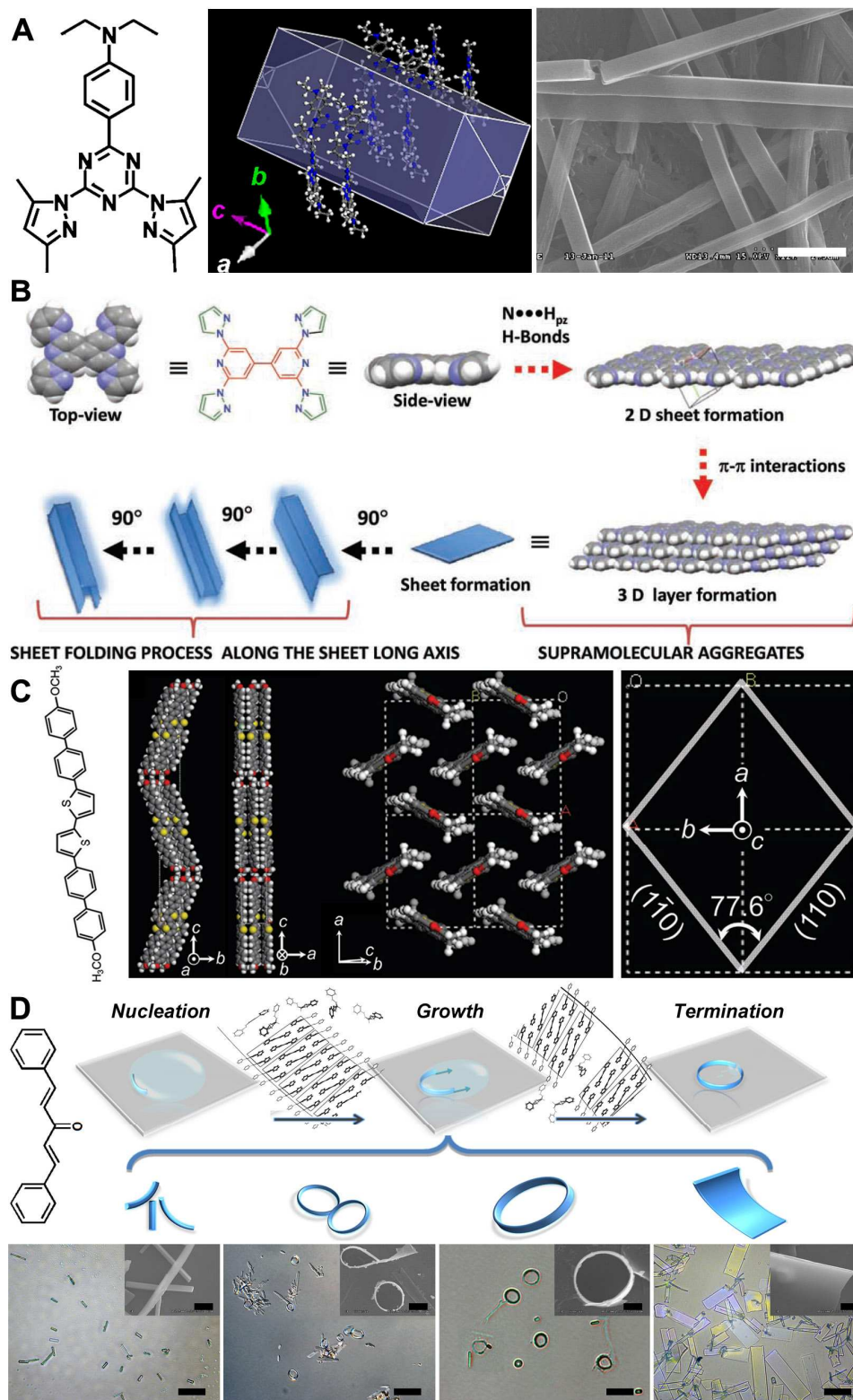


Fig.2 Formation mechanisms of four representative structures. (A) Nanowire: (left) Molecular structure of DBPT; (middle) Predicted growth morphology of DBPT crystalline structure; (right) SEM image of the DBPT nanowires. Scale bar is 2 μm . (B) Schematic elucidation of the possible formation

mechanism of tubular structures via supramolecular self-assembly of 2,6-di-pyrazol-1-ylpyridine. (C) Nanosheet: (left) Molecular structure of BP2T-OMe; (middle) Crystal structures of BP2T-OMe with projections of *bc*-plane, *ac*-plane, and herringbone packing mode along the *c* axis, respectively; (right) Crystal lattice in the *ab*-plane. (D) Microring: (up) Molecular structure of DPPDO and illustration of self-assembling mechanism of microrings; (bottom) Optical microscopy images of nanowires, small/large rings and tiles by using DPPDO solutions with different concentrations. Scale bars are 25 μm . Insets show the corresponding SEM images. Scale bars are 2 μm . Figure 1A, Copyright 2011, American Chemical Society; Figure 1B, Copyright 2011, Wiley; Figure 1C, Copyright 2012, Wiley; Figure 1D, Copyright 2013, Wiley

Figure 2C shows the molecular pattern in the low-dimensional crystals with a consequent rhombus shape.¹⁵ This model compound, 5,5'-bis(4'-methoxybiphenyl-4-yl)-2,2'-bithiophene (BP2T-OMe), has a long chain core of thiophene/phenylene co-oligomer (Figure 2C left), which has been widely used as gain media for lasing. It can be observed from the middle of Figure 2C that the molecules are tilted against the *ab*-plane, which is governed by the interactions between methoxy groups. The molecular axes are alternately declined in the opposite direction to the *c*-axis in the stacked molecular layers because of the zigzag molecular shape. A classic herringbone packing is clearly observed when projected along the molecular axis in one molecular layer in parallel to the *ab*-plane. It is the combination of π stacking and interactions between peripheral methoxy groups that are responsible to the formation of the two-dimensional shape, because hydrogens on the molecular terminals do not contribute to the stabilization of an orthorhombic form.¹⁶ The angle between the (110) and (1 $\bar{1}$ 0) faces of the crystal is determined to be 77.6°, which is close to the edge angle of the rhombus shape of the sheet.

Recently, our group succeeded in a controllable construction of microrings with an organic compound named 1,5-diphenyl-1,4-pentadien-3-one (DPPDO).¹⁷ The molecular structure of DPPDO is displayed in Figure 2D. This molecule enables a rearrangement in the loose crystal lattice due to a good tolerance for structural distortion. The molecular planes are perpendicular to the *c* axis and the distance between neighboring molecules along *c* axis is a bit large, revealing a buffer space for the movement of DPPDO molecules. As a result, the self-assembled DPPDO 1D structures are of remarkable flexibility, which implies a bendable characteristics in the preferential growth directions. Therefore, it is capable to achieve self-assembled microrings from the aggregation of DPPDO molecules, as long as an appropriate driving force could be applied for the circular growth during the assembly process.

In this work, the crystalline microrings were fabricated by introducing the liquid tension of solution droplets during the self-assembly process. The DPPDO molecules concentrate preferentially first at the contact line between micro-sized droplet and substrate, where the solvent evaporated faster than that in the central area. The solution droplet was therefore confined within the inner surface, and offered a circular template for the assembly around the droplet. As DPPDO segments grow large, molecular packing bends gradually induced by the force of liquid tension at the contact line. With the further evaporation of solvent, the segments grow into a curved belt. The formation of the rings greatly depends on the amount of DPPDO units in the microdroplets (Figure 2D bottom). If there are no sufficient molecules, only short rods would emerge. With the increase of DPPDO amount, the products gradually develop into incomplete and perfect microrings. However, only large tiles appear if there were excess DPPDO in a droplet, because of the huge mechanical resistance needed to be overcome for the wide tiles. From this instance, we can infer that though intermolecular forces dominate the self-assembly behavior and thus the final morphology, other influences, such as amount,¹⁸ should not be ignored.

2.2 Influences of external factors

Besides inherent intermolecular force, some other external conditions from environments, solvent, humidity,¹⁹ surface tension, temperature,²⁰ aging time²¹ and ultrasonic action,²² etc, also take an effect in determining the packing behavior of molecules. For example, a highly humid condition would be crucial to the formation of self-assembled structures with ring shape for thiocyanine derivatives.¹⁹ Zhang and colleagues reported that by changing the process temperature, three kinds of single crystal nanostructures, that are nanoribbons, nanotubes, and nanowires, can be controllably prepared with a single intramolecular charge-transfer organic compound.²⁰

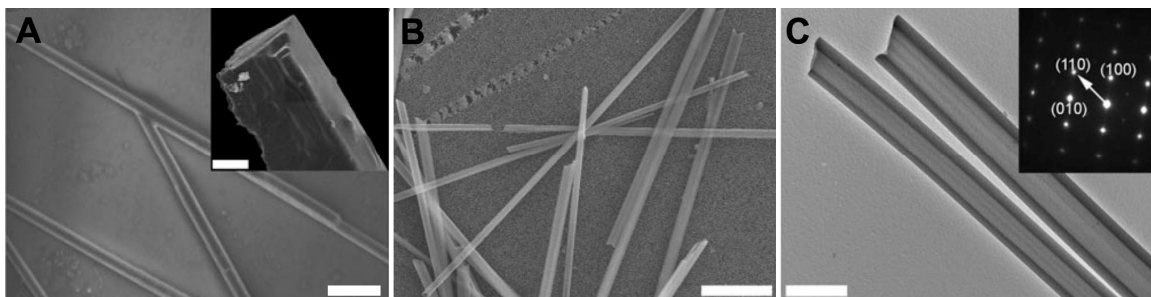


Fig.3 Solvent etching effect on the self-assembled structures. (A) SEM image of the BPEA microrods prepared with a regular liquid phase self-assembly. Scale bar is 5 μm . Inset: SEM image of a single rod tip. (B) SEM image of BPEA microtubes prepared through an assembly process under reflux. Scale bar is 10 μm . (C) TEM image of the typical BPEA microtubes. Scale bar is 2 μm . Inset: SAED pattern. Copyright 2008, Wiley.

2.2.1 Solvent effect in self-assembly

Figure 3 illustrates an example of solvent effect on the products with distinct morphologies, i.e. solid rods and hollow tubes,

respectively. Both the structures were formed by the self-assembly in liquid phase.²¹ Briefly, 9,10-bis(phenylethynyl)anthracene (BPEA) solution was injected into boiling water under vigorous agitation and then cooled to room

temperature. Figure 3A shows the SEM image of the obtained microrods and the magnified image of a single rod tip. If the boiling system was kept refluxed for a period before cooling, the final products would be perfect hollow tubes (Figure 3B), which were further confirmed by the TEM image (Figure 3C). Two structures have the same preferential growth direction of [001] (Figure 3C inset). The reason why reflux enables the formation of hollow structure was explored through a variation of reflux time. It is the etching of BPEA molecules by the small amount of ethanol (the good solvent) during the reflux period that resulted in the formation of the hollow tubular structures.²³

2.2.2 Site-selected self-assembly on specific substrates

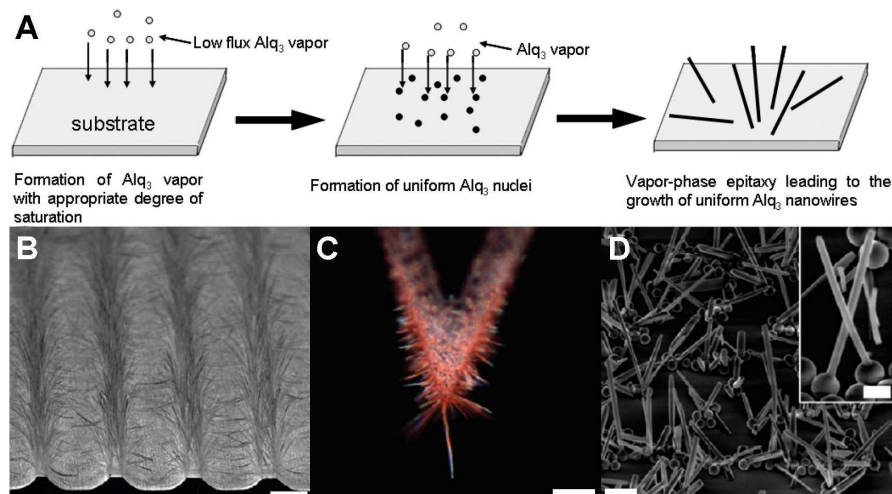


Fig. 4 Substrate effect on the self-assembly of organic molecules in vapor phase. (A) Growth mechanism of Alq₃ nanowires with the assistance of adsorbents to improve the uniformity and crystallinity. (B) Patterned growth of DAAQ nanowire arrays on silicon wafers with periodic ridge-groove patterns. Scale bar is 25 μm. (C) Optical microscopy image of the DAAQ nanowires grown at an AFM tip. Scale bar is 10 μm. (D) SEM image of the DAAQ nanowires grown on silica spheres. Inset is the magnified image. Scale bars are 2 μm. Figure A, Copyright 2006, Wiley; Figure B-D, Copyright 2010, American Chemical Society.

It was found that the introduction of adsorbent in vapor phase deposition improves the quality remarkably.²⁵ The adsorbents, which can be neutral aluminum oxide or silica gel, are extremely helpful to control the degree of supersaturation. The mechanism is considered to be the existence of an adsorption-desorption equilibrium between the adsorbents and the organic sources. A series of crystalline organic nanostructures have been prepared with this improved method. Figure 4A illustrates a typical self-assembly process of tris(8-hydroxyquinoline)aluminum (Alq₃) compound. Here a mixture of Alq₃/adsorbent was used as material source and heated to the deposition temperature. The sublimed Alq₃ vapor with appropriate degree of supersaturation translates into small Alq₃ crystal nuclei with high uniformity on the substrates. Then subsequent Alq₃ molecules adsorbed onto the nuclei through intermolecular interactions and self-assembled into uniform 1D nanowires.

Assembling 1D structures into vertically aligned arrays has been actively pursued because of the advantages for wide applications, such as solar cells, batteries, light emitting diodes, and so forth. Previous reports on array materials mostly concentrated on inorganic semiconductors²⁶ or material fabricated through various templates.^{27, 28} Since organic division has been widely used in photoelectric area, it is necessary to acquire organic nanowire arrays. Huang *et al.* reported a direct growth of vertically aligned

For self-assembly in liquid phase, the solvent is of great significance because that some other external factors come into play through it, such as temperature, solubility, aging time and surface tension. By contrast, the most important factor for self-assembly in vapor phase is the parameters of vaporized organic molecules. It is well known that the supersaturation degree of the vaporized molecules is the key factor in deciding the morphology and monodispersity.²⁴ Maintaining the vapor saturation at a low level will facilitate the process of most organic materials into uniform low-dimensional structures. Thus, it is increasingly important to be able to control such a parameter.

organic nanowire array with 1,5-diaminoanthraquinone (DAAQ).²⁹ It was found that DAAQ tends to preferably nucleate and grow faster on high surface energy sites. This site-selected growth enables a patterned growth on substrates with specific treatment. Figure 4B is the tilted view SEM image of DAAQ arrays grown on a silicon substrate modified with alternating ridge edges and grooves. Here, DAAQ molecules selectively nucleate and grow on ridge edges with a high surface energy. Similarly, DAAQ molecules could also grow on AFM tips (Figure 4C) with a much longer nanowire near the very end tip, where possesses the highest surface energy. This reminds us that introducing extra sites with high surface energy should be an effective way to control the distributions of the obtained nanostructures. It has been proved that the size of grow site affects the number and orientation of DAAQ nanowires. As demonstrated in Figure 4D, only one nanowire grew on each silica sphere with a proper diameter of 520 nm. The ease of the oriented vertical growth and modulation provides convenience for the fabrication complex structures as well as direct integration of nanowires into devices.

3. From self-assembly to structures

One of the most important reasons why organic nanostructures become so attractive is the fact that their optical and electronic

properties are quite different from the inorganic counterparts. As we know, the optical performances are determined by both the intrinsic properties of molecules themselves and the optical confinement effect deriving from the various structural features.

Organic aggregates self-assembled from small molecules are usually crystals with regular shape, where the ordered molecular arrangements could offer good photon confinement. It can be seen from the last section that the molecular self-assembly behaviors directly determines the final structures of tiny crystals. That is to say, the acquisition of distinct structures can be reasonably expected through a finely controlled self-assembly process. In this part, we will discuss the achievements of nanomaterials with specific structures either through rational molecular design or construction condition selection.

3.1 Structure control through intermolecular interactions

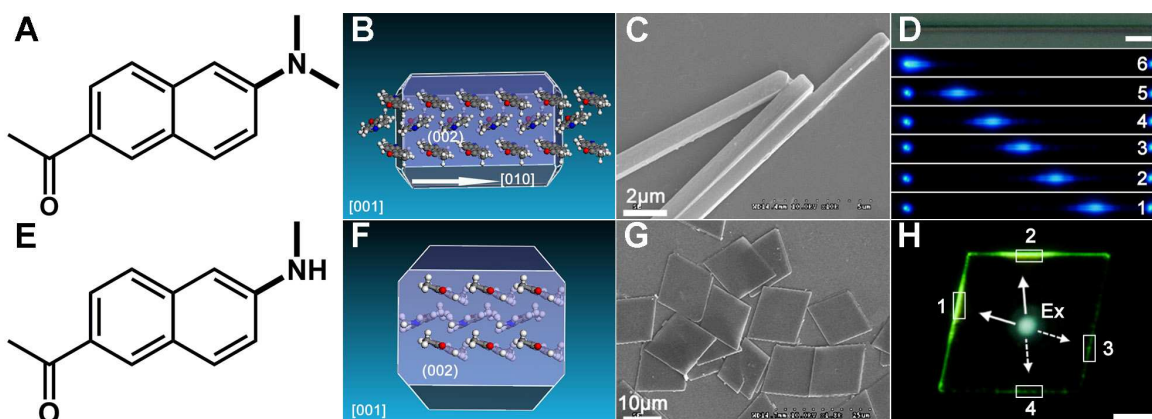


Fig. 5 Self-assembled materials with 1D, 2D structures through molecular design. (A, E) Molecular structures of ADN and AMN, respectively. (B, F) Predicted growth morphologies based on the attachment energies of ADN and AMN molecules. (C, G) SEM images of 1D nanowires aggregated from ADN and 2D rhombic plates from AMN molecules. (D, H) Distinct waveguide behaviors of 1D, 2D structures. Scale bars in D, H are 5 μm and 10 μm , respectively. Copyright 2013, Wiley.

3.1.1 Controlling the structures with molecular design

Very recently, we constructed 1D and 2D nanoarchitectures with distinct photonic confinements through self-assembly by altering the structures of the components, affording a guideline to the molecular design and morphology control (Figure 5).³⁰ The only difference between 2-acetyl-6-dimethylaminonaphthalene (ADN, Figure 5A) and 2-acetyl-6-methylaminonaphthalene (AMN, Figure 5E) is the substituents on the naphthalene core. The secondary amine in AMN could provide less steric repulsion with neighboring molecules and an extra hydrogen-bonding site, preventing packing along a single direction. It is known from the predicted pattern modes (Figure 5B and 5F, respectively) that the thermodynamically stable morphology for ADN is wire-like, while AMN molecules would be arranged in a slip-stack mode and a sheet-like structure induced by the hydrogen bond between adjacent molecules should be obtained.

The 1D growth of ADN (Figure 5C) was determined to be along [010] direction, which can be attributed to the π interactions. These nanowires can serve as active waveguides that the emitted light are confined in the nanowire and propagates along the axis in two predominant directions (Figure 5D). No obvious light loss was observed from the light intensities for position 1-6 (labeled in Figure 5D) with the increase of propagation length, indicating a low-loss transmission. Similarly, the growth directions of the 2D

We have known that molecules would self-assemble into various structures if appropriate forces were introduced during the aggregation process. Since the optical performances are strongly morphology-dependent, a controllable synthesis is of particular significance. In most cases, aromatic molecules tend to self-assemble into one-dimensional structures through strong π - π interaction if there are no other intermolecular interactions. Modifying molecular structure by tailoring the constitute groups may introduce additional forces and disturb the balance of π stacking, causing different preferential growth patterns, such as direction, planarity and steric hindrance effect. Thus, the rational design of molecular components with different intermolecular recognitions would be promising for the acquisition of nanostructures with desired morphologies, which can manipulate photons in specific modes.

rhombic sheets (Figure 5G) are [100] and [010], which are related to the π - π interaction and hydrogen bond interactions, respectively. When a laser beam was focused at the center of the rhombus plate, the neighboring two outcoupled edges (marked with 1 and 2, Figure 5H) have large, bright emissions, which shows significant contrast with the small, obscure outcouplings at the opposite edges (3 and 4). The intensity difference between edges of an acute angle implies an asymmetric light propagation, which may play a fundamental role in creating new types of devices.

For organic compounds, not only the kind and steric hindrance of substituent groups,^{19, 31} but also their positions may significantly influence the dominant driving forces in self-assembly process, and thus the appearance of final products.³² It has been demonstrated that three isometric molecules of bis(iminopyrrole)benzene could self-assemble into well-defined spheres, wires and cubes, respectively, though the intermolecular forces are the same. It is the different interactions for aggregate stacking at supramolecular level caused by the isomeric molecular structures that is most likely responsible for the different morphological evolution.

3.1.2 Structures obtained from the synergistic assembly of different compounds

Intermolecular interactions between different compounds can be

utilized to get multicomponent structures through their cooperative self-assembly.³³ The selected compounds usually constitute a donor-acceptor pair with high energy transfer efficiency, where a small amount of energy acceptor would quench the donor emission heavily. In organic binary aggregates, the energy transfer process through either dipole-dipole interaction or electron-exchange mechanism would be very effective due to the reduced intermolecular distance, affording an alternative way to obtain tunable color emission. Benefit from the fruitful excited state dynamics, the doped structures could not only maintain the advantages of each component, but also provide novel optical performances, for example, white light emission.³⁴ Therefore, exploitation of construction strategy to complex systems has a far-reaching consequence to the overall manipulation of photon parameters.

Figure 6 shows two typical 1D binary structures self-assembled through the recognitions of different molecules. The well-defined nanowires shown in Figure 6A were prepared with the above mentioned adsorbent-assisted epitaxial growth method with a blue light emitter (1,3,5-triphenyl-2-pyrazoline, TPP) and an orange dye (rubrene) as the deposition sources. The distribution of the dopant was determined to be uniformly embedded in the TPP host. These two dyes constitute a good host-guest pair of Förster resonant energy transfer (FRET). The emission color varies a lot along with the rubrene doping content, which was tuned by changing the molar ratio of the source materials. When a proper TPP/rubrene molar ratio (100:1) was adopted, white light emission can be achieved from these 1D nanostructures. The emission color evolution from blue to orange is shown in Figure 6B. At first, there was only one characteristic fluorescence band for pure TPP nanowires. With the increase of rubrene content, the emission of TPP was quenched gradually, while the emission corresponding to the rubrene rose up rapidly. At a proper doping ratio, a stable white light was observed.

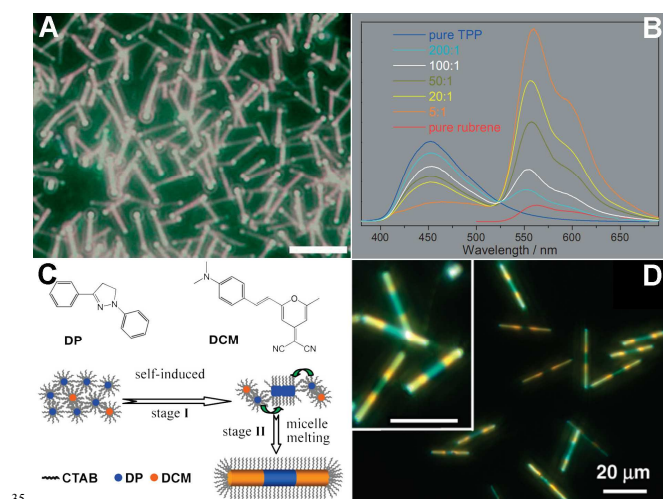


Fig. 6 Composite structures fabricated from the synergistic assembly of different molecules. (A) PL microscopy image of TPP/rubrene nanorods with controllable doping ratios. Scale bar is 5 μm. (B) Emission spectra of the TPP/rubrene nanostructures of different doping contents. (C) Molecular structures of DP and DCM as well as the illustration for formation mechanism of the gradiently doped microrods. (D) PL microscopy image of the microrods under UV illumination. Figure A-B, Copyright 2008, Wiley; Figure C-D, Copyright 2010, American Chemical Society.

Yao and co-workers demonstrated a supramolecular synthesis of triblock microrods constituting 1,3-diphenyl-2-pyrazoline (DP) and 4-(dicyanomethylene)-2-methyl-6-(*p*-dimethyl-aminostyryl)-4H-pyran (DCM),³⁵ as illustrated in Figure 6C. With the assistance of cetyltrimethylammonium bromide (CTAB) micelles, the DCM molecules selectively doped at both ends of DP rods. During the self-assembly process, DP molecules first dissolved into the hydrophobic core of the spherical CTAB micelles due to the solubilization effect (stage I). The dissolution of DP molecules helps to the formation of rod-like micelles which then act as templates directing the primary growth of DP molecules. Finally, DCM molecules co-deposited with DP molecules, generating the triblock microrods (Figure 6D). Though these microrods exhibit microarea heterogeneity, they show macroscopic high quality white light emission properties.

3.2 Structure modulation through external factors

We have come to know that self-assembly process can be influenced by environmental factors from the above discussions. Utilizing this, we could intervene in the molecular behavior by adjusting the self-assembly conditions on the basis of a clear aggregation picture. For fac-tris(2-phenylpyridine) iridium (Ir(ppy)₃) compound, the rod and wire structures self-assembled from solvent exchange and solvent-evaporation methods respectively, are of different crystalline form.³⁶ Reversible nanostructure conversion from nanospheres to nanorods and nanoslices have also been realized with the destruction of the axial coordination interaction by the competition of solvent.³⁷

3.2.1 Structures versus aging time

Recently, a reversible shape-shifting of 1,4-bis(1,2':6',1''-bis(3-butyl-1H-3,4,5-triazolyl)pyridin-4'-yl)benzene nanostructures was reported by Chandrasekar group, as shown in Figure 7A.³⁸ The rod-shaped arrangement of three aromatic rings in the molecule center (Figure 7A) ensures a nice molecular planarity. Furthermore, the triazole ring nitrogen atom (N2) participates in two hydrogen bond interactions with phenyl ring protons, which play a vital role in the supramolecular ordering and self-assembly into rectangles sheets (Figure 7B). Those plates, with typical size of micrometers, could switch into tubes (Figure 7C) via a rolling mechanism in the presence of water, while sonication could induce the transformation of the tubes back into plates. The rings were obtained from the tube solution after a week and the transformation process is irreversible.

The absence of any external interference during the whole morphology evolution suggests that the critical activation energy needed to overcome the intermolecular binding forces is very low. For this case, the driving force behind the structural deformation was ascribed to the hydrophobic surface effect, which propels these structures to curve to avoid the exposure to water. Anisotropy optical waveguide was observed with the excitation of a focused laser beam, demonstrating a possibility of switching the wave guiding behavior through light propagating direction in both 1D (Figure 7E-F) and 2D (Figure 7G) structures. This work announces again that various optical performances for different application can be achieved even from the same compound as long as an appropriate fabrication method is pre-designed. Before that, a careful analysis of relationship between intermolecular/environmental interactions and structures

is indispensable to choose proper self-assembly strategies.

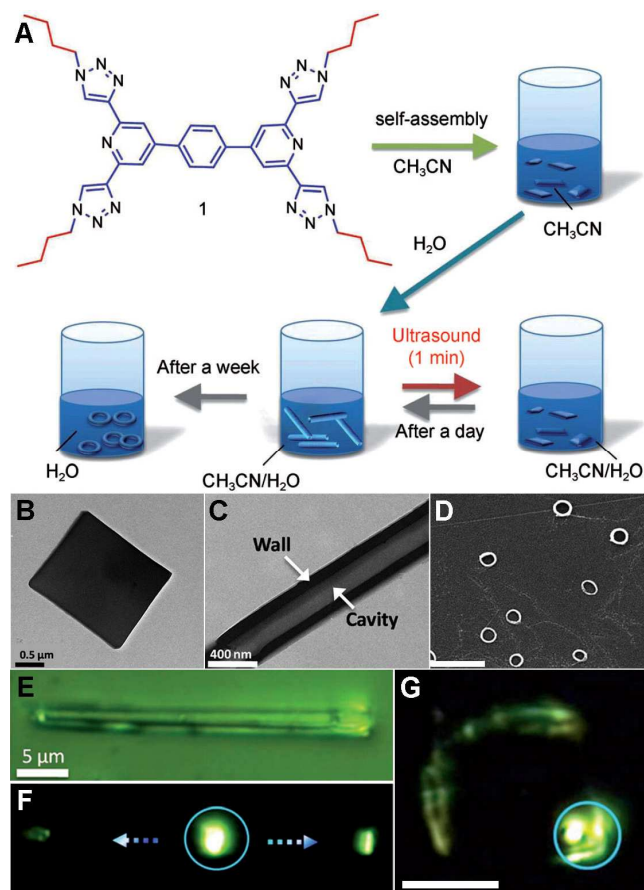


Fig. 7 Various self-assembled nanostructures and corresponding optical properties obtained with different assembly conditions. (A) Sketch map of formation of 2D rectangle plates, 1D nanotubes and 0D nanorings of the compound under different conditions. (B) TEM image of a single rectangle plates. Scale bar is 0.5 μm . (C) TEM image of a single nanotube. Scale bar is 400 nm. (D) SEM image of the nanorings. Scale bar is 2 μm . (E, F) Optical bright-field and photoluminescence microscopy images of an identical microtube. (G) Photoluminescence microscopy image of a single nanosheet with a laser excitation at the corner. Copyright 2012, Wiley.

3.2.2 Heterostructures through site-specific epitaxial growth

As is mentioned above, the site-specific nucleation characteristics of organic molecules could be used to fabricate some useful complex structures, for example organic-metal nanowire heterojunctions, which was realized by our group recently via the vapor deposition of organic compounds on silicon substrates dispersed with pre-fabricated silver nanowires (Figure 8).³⁹ Figure 8A shows the SEM images of silver nanowires with convex vertices, which ensure an overwhelming superiority in attracting vaporized BPEA molecules. During the deposition process, the sharp wire tips play the role of nuclei centers for the condensation of BPEA vapor. Finally, BPEA molecules nucleated and grew specifically adjacent to the tips of the silver wires to form heterojunctions (Figure 8B), which is testified by the TEM image of a single BPEA-silver nanowire junction area (Figure 8C).

Shown in Figure 8D and 8E are the bright-field and photoluminescence microscopy images of an identical organic-

silver nanowire heterojunction. Under an excitation of a focused laser beam, both tips of the BPEA nanowire and the joint point emit bright yellow light due to the active waveguide behavior. The red emission, observed from the end of silver nanowire, can be modulated through the polarization of excitation beam, which is attributed to the direct exciton polariton-plasmon coupling. The distinct characteristic of EPs in organic nanowires affords a new way to realize logic operations with an individual heterojunction. This facile step-by-step growth strategy provides a great convenience for incorporating plasmonic modules as practical components into high-capacity photonic circuits.

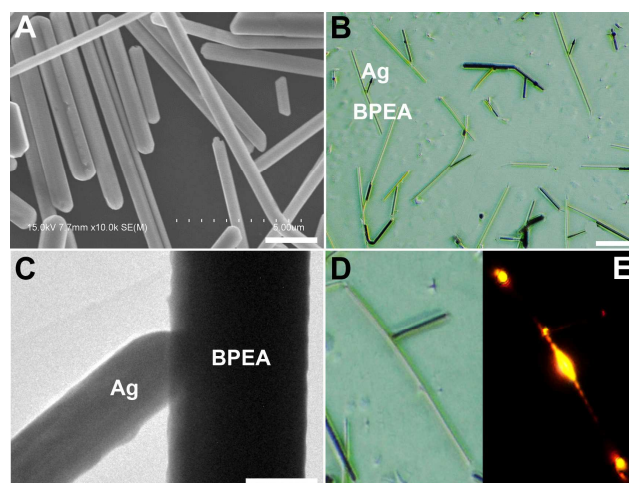


Fig. 8 Preparation of organic-metal nanowire heterojunctions through substrate modification. (A) SEM image of the silver nanowires with convex tips. Scale bar is 2 μm . (B) Optical microscopy image of the BPEA-silver heterojunctions. Scale bar is 20 μm . (C) TEM image of the junction area. Scale bar is 200 nm. (D, E) Optical bright-field and PL microscopy images of an identical junction. Copyright 2012, Wiley.

4. From structures to photonic properties

Low-dimensional structures built from single kind of compound offer an ideal model to investigate the self-assembly characteristics as well as structure-related light confinement as well as electronic properties.⁴⁰ Now we have reached a preliminary comprehending in the relationship among molecule, self-assembly and structures from the last two sections. The rich interactions among different materials, such as energy/charge transfer, exciton migration and conversion, and so forth, might generate a series of novel properties in complex structures. A fine utilization of these new mechanisms would be helpful to the realization of photonic devices with manifold functions.¹¹ Thus, in this part, we will focus on the optical properties and corresponding photonic applications of three representative complex structures self-assembled from organic molecules.

4.1 Nanowire heterojunctions

In comparison with uniformly doped structures, heterostructures would afford a greater flexibility in the manipulations of photons at the micro-/nano- scale. The existence of clear interfaces may give rise to some innovative ways to modulate the light-matter interactions and thus bring out meaningful optical properties. For example, multiple segmented nanostructures exhibit broad multifunctionality in photonic applications, including nanobarcodes,³⁵ p-n junctions,⁴¹ and multiluminescent light

sources. However, these phase-separated low-dimensional structures were mainly prepared via hard template or electrochemical deposition techniques, with a great weakness of amorphous phase. Along with our knowledge on the controllable self-assembly, heterostructures could also be prepared via modulated self-assembly.⁴²

4.1.1 Dendritic heterostructures as optical routers

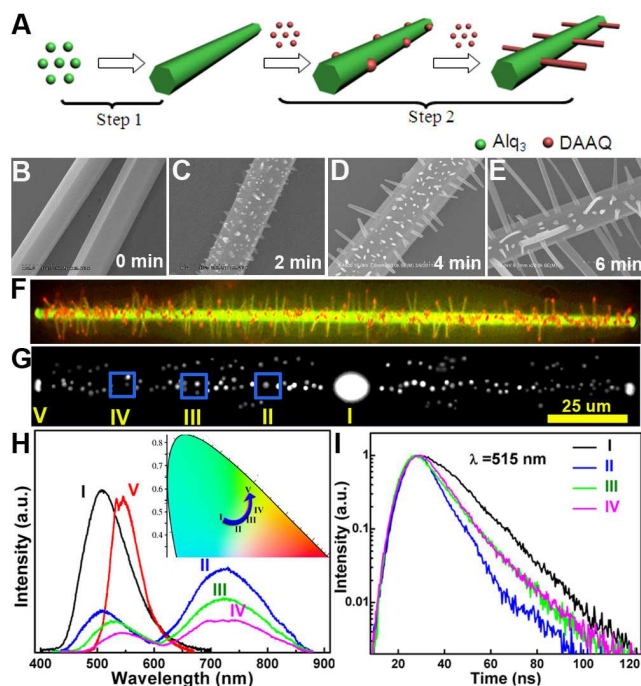


Fig.9 Growth processes and photonic properties of the dendritic organic nanowire heterojunctions. (A) Schematic illustration of the growth processes. Step 1: Alq₃ microwire prepared through self-assembly in liquid phase. Step 2: Site-specific nucleation and epitaxial growth of DAAQ molecules on the Alq₃ microwires. (B-E) SEM images of different growth stages of DAAQ in step 2. (F) PL microscope image of a single nanowire heterojunction under the illumination of unfocused UV light. (G) PL microscope image of the heterostructure under the excitation of a focused laser beam. (H) Spatially resolved photoluminescence spectra of the excited spot (I) and output signals from the DAAQ branches (II-IV) and the Alq₃ tip (V) labeled in G. (I) Photoluminescence decay profiles of Alq₃ emissions at different propagation lengths. Copyright 2012, American Chemical Society.

Organic dendritic structures are concerned due to the potential applications in one-to-many, many-to-one and many-to-many photonic devices. Inspired by the fact that vaporized organic molecules tend to nucleate preferentially and grow more rapidly on sites with smaller curvature radii or higher surface energies,²⁹ we further developed a two-step wire-on-wire deposition method to create organic dendritic structures (Figure 9A).⁴³ Self-assembled crystalline Alq₃ microwire (step 1) with smooth surfaces and hexagonal cross sections (Figure 9B) were used as nucleation centers for the vertical epitaxial growth of DAAQ molecules (step 2). DAAQ molecules nucleate selectively on the Alq₃ microwire to form isolated clusters, seeding subsequent molecular deposition to form the final vertical nanowire branches, which have been proved by the SEM images of different growth stage (Figure 9C-E). Both the branch density and length can be precisely controlled by deposition time and temperature, respectively, illustrating the versatility and

generality of the method. The green emission from Alq₃ trunk and red emission from DAAQ are clearly seen in corresponding positions (Figure 9F), verifying the phase-separated components distribution and existence of clear interfaces.

Those obtained heterostructures can work as optical routers with many output channels that the guided light could be output simultaneously from the trunk tips and each branch under an excitation (Figure 9G). The spatially resolved PL spectra (Figure 9H) from different branches demonstrate propagation-length-dependent outputs as well as color changes (inset). The spectra taken locally from the trunk (curve I and V) show a red-shift due to the variation in the energy transfer efficiency. The other three curves are all superpositions of the green and red emissions from the two compositions, indicating the simultaneous occurring of efficient FRET processes and the direct guidance of Alq₃ emission in DAAQ branches at the interfaces. The decreased fluorescence lifetime of Alq₃ emission at different position (Figure 9H) further proved the energy transfer process.

4.1.2 Nanowire p-n junctions as photoelectric transducers

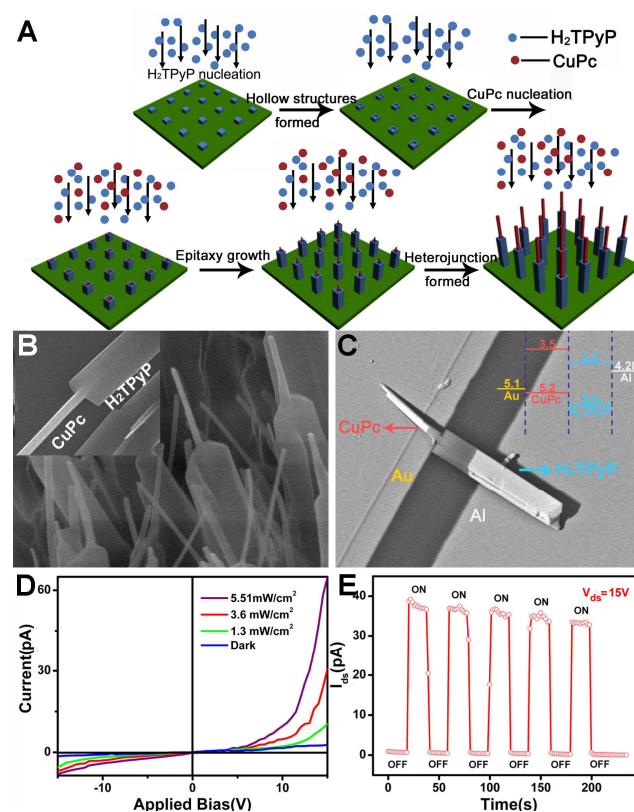


Fig.10 Formation and photoelectric properties of the coaxial organic p-n heterojunctions. (A) Schematic illustration of the self-assembly processes of the CuPc-H₂TPyP p-n junction nanowire arrays. (B) SEM image of the as-prepared nanowire junctions. Scale bar is 1 μ m. Inset shows a single heterojunction. (C) SEM image of a photoelectric device based on a single junction. Inset shows the energy level diagram of the device. (D) Current-voltage (I-V) curves of the device show in (C). (E) Photoswitching characteristics of the p-n junction device. Copyright 2012, Wiley.

If both the nucleation spots and the growth direction can be simultaneously controlled with a high accuracy, where only one wire grows vertically on the predispersed wire, crystalline

heterojunctions would be achieved.⁴⁴ The preparation method could be a two-step way as previously discussed or just one-step, for example co-deposition in vapor phase epitaxial growth, as illustrated in Figure 10A.⁴¹ Here, the p-type material (copper phthalocyanine, CuPc) and n-type material (5,10,15,20-tetra(4-pyridyl)-porphyrin, H₂TPyP) were selected for synthesizing coaxial p-n junction nanowire arrays due to their similar molecular structure. Both compounds were put at different positions of a tube furnace to be co-evaporated with a varied evaporation rate. During the deposition process, H₂TPyP forms vertically aligned hollow structures first, which provide nucleation centers for subsequent CuPc vapor. Then, the two molecules co-deposited onto the substrates to form the heterojunction nanowire arrays (Figure 10B).

The strong π - π interactions between the two planar compounds assures good connections at the junction part which endow each coaxial heterojunction nanowire with great potentials in high-quality optoelectronic device. Figure 10C shows a single device with the prepared p-n junction. Such a device acts as a good photoelectronic transducer, as depicted in Figure 10D and E. The repeatable photocurrent under the light illumination indicates a reversible and stable response to external radiations. The large energy difference between the lowest unoccupied molecular orbital of H₂TPyP and the highest occupied molecular orbital of CuPc at the heterointerface offers a great opportunity for the improvement of device efficiency. Commonly, the larger the wire diameters are, the higher the device efficiency is. Owing to the unique cable-type structure and the large interfacial gap, the single junction device shows better optoelectronic conversion performance than those of single component nanowires and thin film sandwiched devices, which is ready to be applied as highly sensitive photoelectrical transducers in nanoscale photonic circuits.

4.2 Doped nanostructures

In a photonic circuit, the light sources might be nanolaser with a narrow line width or broad band emissions, and even white light, since they provide more possibilities in novel optical signal processing. Doping is a widely used technique in organic materials to obtain color-tunable emissions due to the efficient FRET process. However, the emission colors of the doped materials are usually not stable because of acceptor content variation caused by external stimuli. Therefore, developing a self-modulating mechanism that can adjust the output intelligently, regardless of doping ratio and environmental variation, is necessary and challenging.

4.2.1 Uniformly doped structures as tunable light sources

The combination of FRET down-conversion and triplet-triplet energy transfer (TTET) upconversion in an organic system is supposed to fulfill the requirement. We fabricated uniform 1D nanostructures with 9,10-di-phenylanthracene (DPA) and iridium(III) bis(2-phenylbenzothiazolato-N,C^{2'}) acetylacetonate ((BT)₂Ir(acac)) through self-assembly.⁴⁵ In this composite nanowires, the bi-directional energy transfer that is the FRET from DPA to (BT)₂Ir(acac) and reverse TTET from (BT)₂Ir(acac) to DPA co-exists, rendering the fluctuations of the singlet and triplet excitons during the light propagation. The excitons can fluctuate between the blue emission of DPA and the orange

emission of (BT)₂Ir(acac) in the nanowire. The color ratios of two outcoupling colors from either low or high doped nanowires can reach the same value after the light transmission over a certain distance (Figure 11A), resulting in a self-modulated white light outcoupling at wire tips. Such an optical waveguide behaves like a regulator which converts different input colors into a standard output, in spite of the doping ratio, as displayed in Figure 11B. These results provide a comprehensive understanding of exciton polariton conversion in active waveguiding and effective strategies for developing novel multi-component waveguide building blocks.

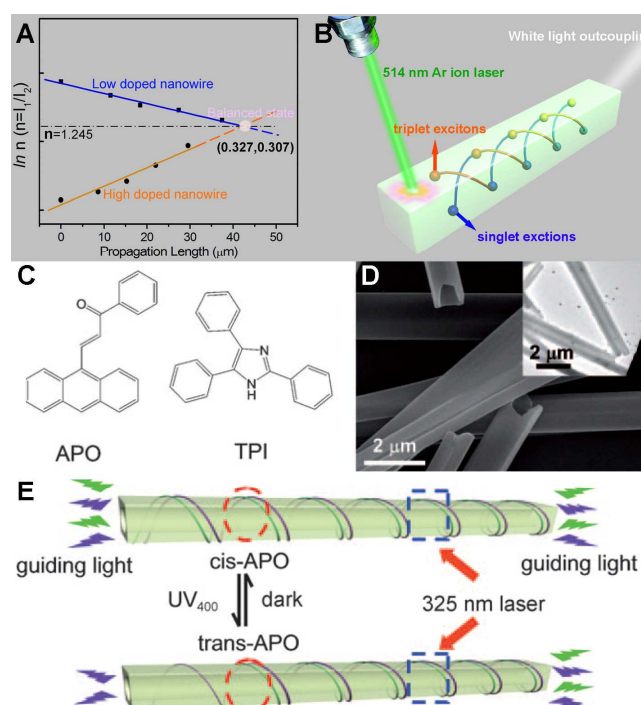


Fig. 11 Fabrication of uniformly doped structures for light sources with tunable emission colors. (A) The exponential relationship between the contribution ratio of donor to acceptor emission, n , and the propagation length in the low and highly doped nanowires. (B) Schematic illustration of mechanism for the self-modulated white light outcoupled emission. (C) Molecular structures of APO and TPI. (D) SEM and TEM (inset) images of the 1D doped tubular structures. (E) The principle of the microtubes as optical waveguide switch. The circled areas represent the photo-isomerization regions induced by UV irradiation. The squares indicate the excited spots for waveguide measurement. Figure A-B, Copyright 2011, Wiley; Figure C-E, Copyright 2011, Wiley.

Optical switcher is an indispensable element to perform some ordinary functions. The achievement of ON/OFF state for photons is not an easy thing because external activities can hardly intervene in the movement of photons. Fortunately, light-matter interactions as well as optical confinement in different structures could be used to solve the problem. Organic molecules, which were endowed with various photo-responses, could be finely utilized to realize specific functions. Here, photochromism,⁴⁶ a reversible change in absorption band modulated by the light irradiations was chosen to construct a kind of waveguide switcher.⁴⁷ Figure 11C presents the molecular structures of a photochromic molecule 3-(anthracen-10-yl)-1-phenylpropan-2-one (APO) and 2,4,5-triphenylimidazole (TPI). Homogeneous tubular structures (Figure 11D) were obtained through the

cooperative assembly of the two model compounds mediated by hydrogen bond.

Under the excitation of a focused laser at the squared area (Figure 11E), the 1D tube would emit intense fluorescence and self-guide to both tips. After the illumination of UV400, the intensity decreased dramatically while the emission with a peak of 540 nm disappeared completely. In the meanwhile, no change was observed in the outcouplings from the right tip before and after the UV irradiation. That is to say, selective switching of the waveguide had been successfully achieved in such a binary tube. The out-coupled light can be turned on again by keeping the sample in the dark. This switch behavior can be reversibly switched over several cycles without any fatigue, demonstrating a good repeatability as reliable photonic devices. This work also enlightens a way to remote control of waveguide behavior through the particular properties of molecules.

4.2.2 Gradiently doped structures as photonic transistors

Precisely design and fabricate chemical heterogeneous structures is another good alternative route to assume specific photonic functions. Benefit from the flexible fabrication through cooperative self-assembly, the spatial excitonic emission during the path of light propagation could be finely engineered through the donor-acceptor energy transfer in organic heterogeneous composites. A template-free method for heterostructures with axially tunable compositions was developed by Zhao and co-workers.⁴⁸ The intermolecular interactions along the growth direction were properly designed between the host and the guest to acquire axial segments. In this work, TPI was selected as the host molecule and another two molecules, a sphere-like organometallic complex $(BT)_2Ir(acac)$ and a planar molecule BPEA were chosen as two typical guest molecules. In the assembly process (Figure 12A), TPI molecules quickly concentrate and nucleate into short rod-like hollow structures and then the guest molecules start to insert into the TPI host matrix subsequently. The sharp contrast between the two molecules lies in the host-guest interactions strength, i.e. the π - π interaction force in BPEA-TPI pair is much stronger than the Van der Waals force in $(BT)_2Ir(acac)$ -TPI. Such a divergence results in the uneven doping of guest component in axial direction.

For $(BT)_2Ir(acac)$, the complete mismatch with TPI in molecular structures brings a large steric hindrance, which terminates the further growth of TPI. Therefore, the final products were characterized as three blocks, with two doped orange blocks as the ends (Figure 12B). Comparatively, the parallel packing of BPEA and TPI molecules with a strong π - π interaction ensures a better molecular compatibility, which allows for the packing of TPI molecules. The consumption of BPEA ends up its aggregation, and then the growth of TPI will be predominating. With the continuous evaporation of solvent, BPEA aggregates again along the 1D growth direction. These processes took place repeatedly until the depletion of molecules. This alternant growth of TPI and BPEA resulted in the multiblock structures with tunable colors (Figure 12C).

This cooperative assembly strategy can be generalized and expanded to achieve some practical functions, such as full-color emission in a single tube¹⁴ or triode for signal processing.^{41, 49} Soon afterwards, 3-(2-benzothiazolyl)-7-diethylaminocoumarin (Coumarin 6) was adopted as the guest compound to acquire

nanostructures with distensible color range on the basis of above results. Besides the intrinsic green emission from monomer, the Coumarin 6 also emits red fluorescence from the charge-transfer state in aggregates, as proved in Figure 12D. Therefore, RGB colors in an individual luminescent structure were accomplished in the TPI-Coumarin 6 pair via controllable doping during the self-assembly.

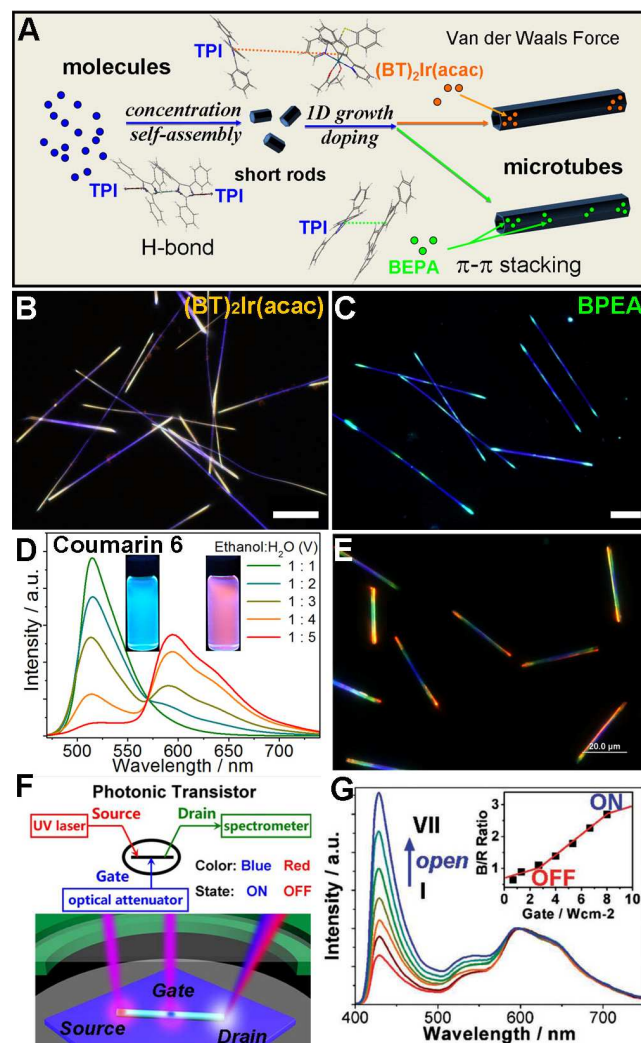


Fig. 12 Formation and optical properties of the gradiently doped 1D nanostructures. (A) Schematic illustration for the formation of doped TPI tubes with different guest molecules. (B, C) PL microscopy images of the triblock and multiblock doped TPI microtubes. (D) Fluorescence spectra of Coumarin 6 aggregates of different contents in the ethanol/water mixture. (E) PL microscopy image of Coumarin 6 doped TPI microtubes. (F) Schematic illustrations of design concept (top) and realization (down) of a photonic transistor in rainbow colored microtubes. (G) Outcoupled emission spectra from the drain port under various gate control. Inset shows the relationship of outputted blue to red light ratio and the power of the gate laser. Figure A-C, Copyright 2012, Wiley; Figure D-G, Copyright 2013, Wiley.

The formation mechanism of the TPI-Coumarin 6 system is similar to that of the TPI- $(BT)_2Ir(acac)$ pair, and 1D wire-like hollow structures were obtained. The axial doping gradient of Coumarin 6 induced the full-colored visible luminescence along these microtubes (Figure 12E). Upon a UV light excitation, both TPI and Coumarin 6 could be excited and emit fluorescence with

different colors. A part of the emitted fluorescence are confined and guided in the tube in both directions. During light propagation, the energy transfer occurs irreversibly from the donor to the acceptor, ensuring a unidirectional light transfer in the optical materials. Such a characteristic is of great importance to the development of essential photonic devices, especially all-optical diode and triode.

The design concept and experimental verification of a photonic triode are demonstrated in Figure 12F. Similar to an electronic triode, the optical analogy also constitutes source, drain and gate components. The excitation with fixed laser intensity at the left end acts as the source, while the outcoupled light from the right tip is regarded at the drain. The gate beam with different attenuations irradiates at the middle part of the individual tube to control the conducting signal from the source to the drain. The outcouplings from the drain (Figure 12G) is gradually altered from red (Blue/Red <1, OFF) to blue (Blue/Red >1, ON) with the increased gate intensity. The continuous Blue/Red ratio suggests a precise gate-modulate output of the transistor.

4.2.3 Core/sheath structures as photonic sensors

Self-assembled crystalline 1D nanostructures are all active waveguides that the fluorescence can be confined and propagated

along the axis due to the difference in refractive index between organic material and surrounding media, that is mostly the air. Ambient environmental changes could be recorded by the transmitted light in form of the light parameters. Since light transmission is very sensitive to the external conditions, such a mechanism could be applied in the fabrication of ingenious sensors. Figure 13 gives an analogous photonic gas transducer with core/sheath structure, which was fabricated through decorating the single crystalline BPEA nanowire with chemo-reactive bis(2,4,5-trichloro-6-carbopen-toxy-phenyl) oxalate (CPPO).⁵⁰ This core/sheath nanostructure was also fabricated with a cooperative self-assembly process (Figure 13A). The cable-like structures appeared along with the appropriate ratio of BPEA to CPPO content that the BPEA nanowires can be totally wrapped by the dye-doped CPPO shell, as is testified by the TEM image in Figure 13B. The periphery CPPO layer is highly sensitive and selective to the chemical gas of H₂O₂ as a typical chemiluminogenic compound. Such a core/sheath structure could not only retain the high chemical activity of CPPO, but also improve its mechanical and optical properties through the introduction of BPEA molecules in the outer layer.

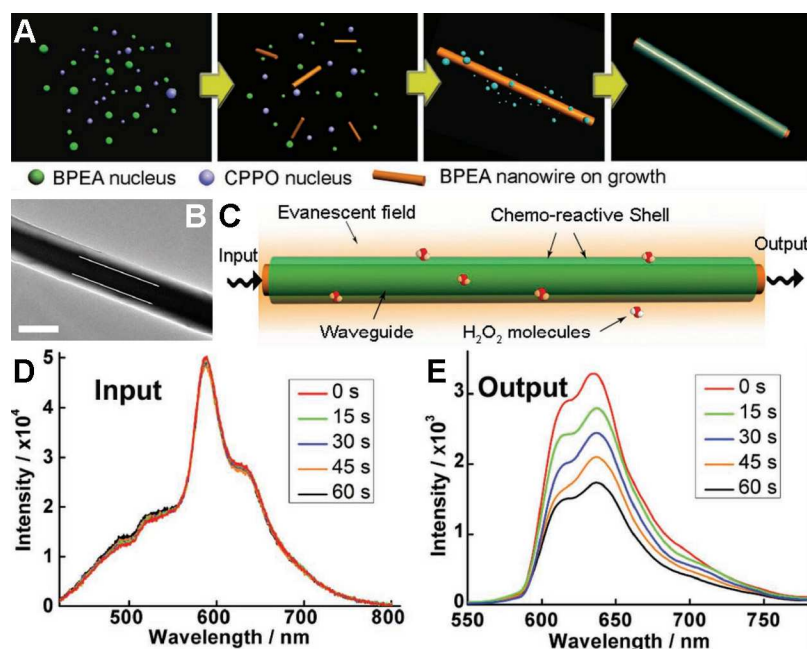


Fig. 13 Formation and photonic sensing performance of the core/sheath nanostructure. (A) Scheme of the growth mechanism. (B) TEM image of a single core/sheath nanowire, Scale bar is 1 μm . (C) Schematic illustration for the evanescent field sensing of the core/sheath optical waveguide. Light is coupled into the cavity and travels through the sensing region coated with chemo-reactive shell. (D, E) Time dependent PL intensities of the input and output light on exposure to 6 ppm H₂O₂ vapor. Copyright 2012, Wiley.

A single core/sheath nanowire was employed for gas sensing based on a gas concentration-dependent evanescent power leakage of a waveguiding nanowire (Figure 13C). The fluorescence under an excitation of a UV laser beam serves as the input signal while the outcoupled light is regarded as the output signal. Once the surrounding media contained trace amount (several ppm) of H₂O₂, the output of the waveguide was drastically attenuated (ca. 50%) with the input intensity remaining unchanged (Figure 13D and 13E). The optical waveguide response of the nanowires exposed to the gas vapors is

remarkably fast (tens of seconds). This cable-like optical waveguide sensing platform complements the present nanowire field-effect sensors with the ability to rapidly and specifically monitor the amplified optical variation across the nanowire waveguiding, showing that a single nanocable is very promising for developing optical probes to detect individual response on chip. The use of a facile self-assembly method to cable-like composites not only bestows the transducer with a defect-free structure and high sensitivity, but also enables the large-scale preparation, which is a key point to commercial products.

5. Conclusions

The ever growing demand of multifunctional photonic devices at micro-/nano-scale greatly promotes the development of chemistry and material. Organic materials have attracted many attentions due to the huge advantages of flexible design, tailored properties, easy processibility as well as low-cost. Small molecules tend to aggregate into low-dimensional crystals under the weak intermolecular interactions, resulting in unique photophysical and photochemical characteristics with large differences from their inorganic counterparts. Obvious structure-dependent photonic properties have been observed these organic nanocrystals, suggesting a way to get desired functionalities. Till now, plenty of construction strategies starting from organic small molecules have been proposed to the acquisition of functional materials with various photonic behaviors.

However, those reports are rather scattered and suffer a high-impact advance, as a systemic studies on the relationships among molecule design, synthesis method selection, morphological modulation and optical performance manipulation of final products. In the aspect, we begin with a comprehensive introduction of self-assembly process of several representative molecules, highlighting the influences from molecular interactions and environmental conditions on the molecular pattern mode. Either aggregation in liquid phase or epitaxial growth in vapor phase has been proved to be universal yet facile preparation method in achieving diverse nanostructures. The careful design and control of self-assembly process have direct impacts on the structural features and corresponding properties of final obtained products.

Rational molecular design and targeted assembly method selection are further steps to function-orientated material synthesis. On the basis of a deep understanding of basic self-assembly rules, we could tailor the intermolecular interactions by modifying the molecular structure or changing the environmental conditions, which may affect both the structures and properties of organic aggregations. A good choice for multifunctional materials is to construct crystalline nanocomposites through cooperative assembly, due to the ease of preparation and flexibility. Multicomponent material, either uniformly or gradiently doped, has been demonstrated to be beneficial for high quality and performance in the integration of the devices. Before that, it is necessary to precisely design and control the structures according to the desired properties. Besides photonic devices, the resultant composite nanomaterials could also be used in biomedicine, sensors, automation, opto-electronics, etc.

So far, the development of organic nanomaterials still falls far behind that of the inorganic category, although considerable attentions have been paid in the past few decades. The preparation of micro-/nano- crystals is still in its early stage. For this reason, a continuous investigation of molecular synergistic self-assembly would be necessary to develop improvements on reproducibility, uniformity, special substrate/organic material requirements, controllable morphology and dimension, and/or crystalline quality. In this sense, we hope to promote a deep understanding of the relationship among molecules, self-assembly, structures and properties through this tutorial review to speed up the spiraling development of organic nanophotonics (Figure 14). Benefit from the present development status, we

have known that distinct optical properties can be achieved through rational molecular design and fabrication strategy selection. New efforts based on current cognitions would keep a higher level and help us to come to a better comprehension of function-oriented self-assembly process as well as structure construction, which would further stimulate progresses in this area. During the process, a reasonable theoretical model, which is not limited to several molecules, will be beneficial for an in-depth knowledge of the aggregation process and structural confinement effect.

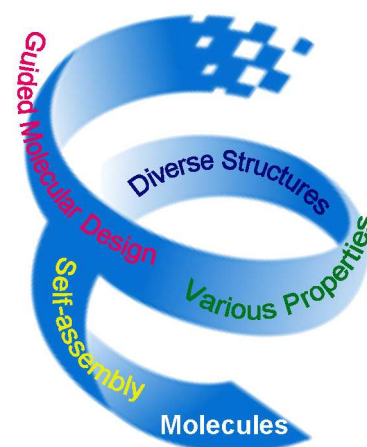


Fig. 14 We hope to promote a spiraling cognition of the relationships among molecules, self-assembly, structures and properties to power the following development of organic nanophotonic materials and devices.

Present photonic devices primarily take advantage of the linear optical properties only, especially light emission. It is difficult to realize some sophisticated applications solely with the linear response, such as ultrafast switcher or signal amplifier. Organic nanostructures with large nonlinear optical coefficients would be an appreciate alternative in such areas. The response time to external inputs is usually on the order of femtosecond to picoseconds. Such a rapid response ensures a good signal processing speed. Moreover, the nonlinear properties of organic materials might be magnified at micro-/nano- scale due to the size-dependent optical confine effect, facilitating the design and realization of nonlinear photonic devices.

Considering the vast number of organic species and great possibilities of their structure-related optical performances, we believe that there will be a brighter perspective for the organic assembles working as a photonic material. To achieve this goal, we need to devote ourselves to further explore this promising field, especially the relationship among molecule, morphology and function. There are still many challenges, *e.g.* synthesis of hierarchical structures, acquisition of complex functions, synergistic effects among different compositions, and so on. We expect the bottom-up assembly method to open up a new prospect for the creation of novel photonic materials.

Acknowledgements

This work was supported by the National Natural Science Foundation of China (Nos. 21125315, 21373241), the Ministry of

Science and Technology of China (2012YQ120060), and the Chinese Academy of Sciences.

Notes and references

^a Beijing National Laboratory for Molecular Sciences (BNLMS), CAS Key Laboratory of Photochemistry, Institute of Chemistry, Chinese Academy of Sciences, Beijing, China. Fax: 86-10-62652029; Tel: 86-10-62652029; E-mail: yszhao@iccas.ac.cn

1. R. Kirchain and L. Kimerling, *Nat. Photon.*, 2007, **1**, 303.
- 10 2. B. Piccione, C.-H. Cho, L. K. van Vugt and R. Agarwal, *Nat. Nanotechnol.*, 2012, **7**, 640.
3. J. Clark and G. Lanzani, *Nat. Photon.*, 2010, **4**, 438.
4. Y. S. Zhao, H. Fu, A. Peng, Y. Ma, Q. Liao and J. Yao, *Acc. Chem. Res.*, 2009, **43**, 409.
- 15 5. Y. S. Zhao, H. Fu, A. Peng, Y. Ma, D. Xiao and J. Yao, *Adv. Mater.*, 2008, **20**, 2859.
6. A.-J. Avestro, M. E. Belowich and J. F. Stoddart, *Chem. Soc. Rev.*, 2012, **41**, 5881.
7. J.-M. Lehn, *Science*, 2002, **295**, 2400.
- 20 8. C. Cordovilla and T. M. Swager, *J. Am. Chem. Soc.*, 2012, **134**, 6932.
9. Y. Hong, J. W. Y. Lam and B. Z. Tang, *Chem. Soc. Rev.*, 2011, **40**, 5361.
10. Y. Yan and Y. S. Zhao, *Adv. Funct. Mater.*, 2012, **22**, 1330.
11. Y. Yan, C. Zhang, J. Yao and Y. S. Zhao, *Adv. Mater.*, 2013, **25**, 3627.
- 25 12. L. Zang, Y. Che and J. S. Moore, *Acc. Chem. Res.*, 2008, **41**, 1596.
13. C. Zhang, C.-L. Zou, Y. Yan, R. Hao, F.-W. Sun, Z.-F. Han, Y. S. Zhao and J. Yao, *J. Am. Chem. Soc.*, 2011, **133**, 7276.
14. S. Basak and R. Chandrasekar, *Adv. Funct. Mater.*, 2011, **21**, 667.
- 30 15. H. Mizuno, U. Haku, Y. Marutani, A. Ishizumi, H. Yanagi, F. Sasaki and S. Hotta, *Adv. Mater.*, 2012, **24**, 5744.
16. J. Bernstein, J. A. R. P. Sarma and A. Gavezotti, *Chem. Phys. Lett.*, 1990, **174**, 361.
17. C. Zhang, C.-L. Zou, Y. Yan, C. Wei, J.-M. Cui, F.-W. Sun, J. Yao and Y. S. Zhao, *Adv. Opt. Mater.*, 2013, **1**, 357.
- 35 18. L. Huang, Q. Liao, Q. Shi, H. Fu, J. Ma and J. Yao, *J. Mater. Chem.*, 2010, **20**, 159.
19. K. Takazawa, *Chem. Mater.*, 2007, **19**, 5293.
20. X. Zhang, X. Zhang, K. Zou, C.-S. Lee and S.-T. Lee, *J. Am. Chem. Soc.* 2007, **129**, 3527.
- 40 21. Y. S. Zhao, J. Xu, A. Peng, H. Fu, Y. Ma, L. Jiang and J. Yao, *Angew. Chem. Inter. Ed.*, 2008, **47**, 7301.
22. Y. S. Zhao, W. Yang and J. Yao, *Phys. Chem. Chem. Phys.*, 2006, **8**, 3300.
- 45 23. X. Zhang, X. Zhang, W. Shi, X. Meng, C. Lee and S. Lee, *Angew. Chem. Inter. Ed.*, 2007, **46**, 1525.
24. Z. R. Dai, Z. W. Pan and Z. L. Wang, *Adv. Funct. Mater.*, 2003, **13**, 9.
25. Y. S. Zhao, D. Xiao, W. Yang, A. Peng and J. Yao, *Chem. Mater.*, 2006, **18**, 2302.
- 50 26. M. H. Huang, S. Mao, H. Feick, H. Yan, Y. Wu, H. Kind, E. Weber, R. Russo and P. Yang, *Science*, 2001, **292**, 1897.
27. D. O'Carroll, I. Lieberwirth and G. Redmond, *Nat. Nanotechnol.*, 2007, **2**, 180.
28. A. L. Briseno, S. C. B. Mannsfeld, M. M. Ling, S. Liu, R. J. Tseng, C. Reese, M. E. Roberts, Y. Yang, F. Wudl and Z. Bao, *Nature*, 2006, **444**, 913.
29. Y. S. Zhao, P. Zhan, J. Kim, C. Sun and J. Huang, *ACS Nano*, 2010, **4**, 1630.
30. W. Yao, Y. Yan, L. Xue, C. Zhang, G. Li, Q. Zheng, Y. S. Zhao, H. Jiang and J. Yao, *Angew. Chem. Inter. Ed.*, 2013, **52**, 8713.
- 60 31. S. Cantekin, D. W. R. Balkenende, M. M. J. Smulders, A. R. A. Palmans and E. W. Meijer, *Nat. Chem.*, 2011, **3**, 42.
32. Y. Wang, H. Fu, A. Peng, Y. Zhao, J. Ma, Y. Ma and J. Yao, *Chem. Commun.*, 2007, 1623.
- 65 33. S. K. Park, S. Varghese, J. H. Kim, S.-J. Yoon, O. K. Kwon, B.-K. An, J. Gierschner and S. Y. Park, *J. Am. Chem. Soc.*, 2013, **135**, 4757.
34. Y. S. Zhao, H. B. Fu, F. Q. Hu, A. D. Peng, W. S. Yang and J. Yao, *Adv. Mater.*, 2008, **20**, 79.
- 70 35. Y. Lei, Q. Liao, H. Fu and J. Yao, *J. Am. Chem. Soc.*, 2010, **132**, 1742.
36. H. Wang, Q. Liao, H. Fu, Y. Zeng, Z. Jiang, J. Ma and J. Yao, *J. Mater. Chem.*, 2009, **19**, 89.
37. T. Liu, Y. Li, Y. Yan, Y. Li, Y. Yu, N. Chen, S. Chen, C. Liu, Y. Zhao and H. Liu, *J. Phys. Chem. C*, 2012, **116**, 14134.
- 75 38. N. Chandrasekhar and R. Chandrasekar, *Angew. Chem. Inter. Ed.*, 2012, **51**, 3556.
39. Y. Yan, C. Zhang, J. Y. Zheng, J. Yao and Y. S. Zhao, *Adv. Mater.*, 2012, **24**, 5681.
- 80 40. V. Palermo, E. Schwartz, C. E. Finlayson, A. Liscio, M. B. J. Otten, S. Trapani, K. Müllen, D. Beljonne, R. H. Friend, R. J. M. Nolte, A. E. Rowan and P. Samori, *Adv. Mater.*, 2010, **22**, E81.
41. Q. H. Cui, L. Jiang, C. Zhang, Y. S. Zhao, W. Hu and J. Yao, *Adv. Mater.*, 2012, **24**, 2332.
- 85 42. L. Bu, E. Pentzer, F. A. Bokel, T. Emrick and R. C. Hayward, *ACS Nano*, 2012, **6**, 10924.
43. J. Y. Zheng, Y. Yan, X. Wang, Y. S. Zhao, J. Huang and J. Yao, *J. Am. Chem. Soc.*, 2012, **134**, 2880.
44. Y. Zhang, H. Dong, Q. Tang, S. Ferdous, F. Liu, S. C. B. Mannsfeld, W. Hu and A. L. Briseno, *J. Am. Chem. Soc.*, 2010, **132**, 11580.
- 90 45. C. Zhang, J. Y. Zheng, Y. S. Zhao and J. Yao, *Adv. Mater.*, 2011, **23**, 1380.
46. J. Zhang, Q. Zou and H. Tian, *Adv. Mater.*, 2013, **25**, 378.
47. Q. Liao, H. Fu, C. Wang and J. Yao, *Angew. Chem. Inter. Ed.*, 2011, **50**, 4942.
- 95 48. C. Zhang, Y. Yan, Y.-Y. Jing, Q. Shi, Y. S. Zhao and J. Yao, *Adv. Mater.*, 2012, **24**, 1703.
49. C. Zhang, Y. Yan, J. Yao and Y. S. Zhao, *Adv. Mater.*, 2013, **25**, 2854.
- 100 50. J. Y. Zheng, Y. Yan, X. Wang, W. Shi, H. Ma, Y. S. Zhao and J. Yao, *Adv. Mater.*, 2012, **24**, OP194.

5

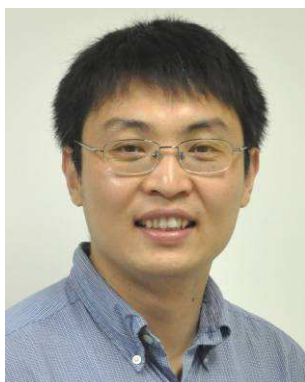


10

15

20

Yongli Yan received her Ph.D. degree in 2008 at Fudan University. Then she joined the National University of Singapore as a postdoctoral fellow. In 2010, she joined Prof. Yong Sheng Zhao's research group as an assistant professor and was promoted to associate professor in 2012. Her research interests are focused on the linear&nonlinear optical properties of organic composite materials, including the controllable synthesis of hybrid materials, comprehensive investigation of the involved energy/charge/exciton processes, and their applications in optoelectronic area.



Yong Sheng Zhao received his Ph.D. degree in 2006 at Institute of Chemistry, Chinese Academy of Sciences (ICCAS). After that, he joined the University of California at Los Angeles (UCLA) and Northwestern University as a postdoctoral fellow. In 2009, he returned to ICCAS as a Professor of Chemistry. His research interests are focused on organic nanophotonic materials and devices, including the controllable synthesis of low dimensional organic materials, comprehensive investigation of the photophysical and photochemical processes involved in the materials, and the design, fabrication and performance optimization of photonic/optoelectronic nanodevices.